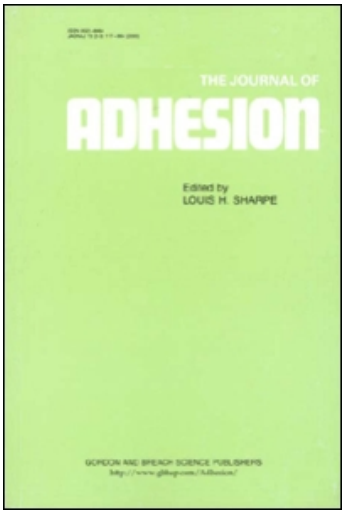

The Journal of Adhesion
Publication details, including instructions for authors and subscription information:
http://www.informaworld.com/smpp/title~content=t713453635

A Stress Singularity Approach for the Prediction of Fatigue Crack Initiation in Adhesive Bonds. Part 1: Theory

D. R. Lefebvre[a]; D. A. Dillard[a]
[a] Engineering Science and Mechanics Department, Virginia Polytechnic Institute and State University, Blacksburg, USA

To cite this Article Lefebvre, D. R. and Dillard, D. A.(1999) 'A Stress Singularity Approach for the Prediction of Fatigue Crack Initiation in Adhesive Bonds. Part 1: Theory', The Journal of Adhesion, 70: 1, 119 — 138
To link to this Article: DOI: 10.1080/00218469908010490
URL: http://dx.doi.org/10.1080/00218469908010490

J. Adhesion, 1999, Vol. 70, pp. 119–138
Reprints available directly from the publisher
Photocopying permitted by license only

A Stress Singularity Approach for the Prediction of Fatigue Crack Initiation in Adhesive Bonds. PART 1: Theory*

D. R. LEFEBVRE† and D. A. DILLARD

Engineering Science and Mechanics Department, Virginia Polytechnic Institute and State University, Blacksburg, VA 24061, USA

(Received 30 May 1998; In final form 17 December 1998)

Since crack initiation in adhesive bonds tends to occur near the interface corners where the stress fields are singular, we define a fatigue initiation criterion using stress singularity parameter, Q (a generalized stress intensity factor) and the singular eigenvalue, λ.

Hattori *et al.*, successfully used a generalized stress intensity factor to characterize the static strength of bimaterial interfaces. We show that this criterion is only appropriate for situations in which the adhesive contact angle is no larger than 90° and the modulus ratio (adhesive to adherend) is smaller than 0.1. Fortunately, these conditions are often met in real joints, permitting the use of a single eigenvalue approach. We then extend this criterion to the case of fatigue arising from mechanical, thermal, or hygroscopic cycling.

In preparation for Part 2 (experimental), the special case of an epoxy wedge on a flat aluminum substrate is considered. The singularity is analyzed both analytically and numerically. The scale of the region dominated by the singularity is found to be of the order of 100 μm. The size of the plastically yielded zone near the apex is found to decrease extremely rapidly as the stress intensity factor goes down, thereby increasing the applicability of the method at the low stress levels often encountered in fatigue.

Keywords: Adhesive bond; fatigue; durability; debond initiation; bimaterial wedge; bimaterial interface; singular stress field; generalized stress intensity factor; plastic zone; spew

*Presented at the 21st Annual Meeting of The Adhesion Society, Inc., Savannah, Georgia, USA, February 22–25, 1998.

†Address for correspondence: Motorola/AIEG, 4000 Commercial Avenue, Northbrook, IL 60062-1840, USA. Tel.: 847-480-8044, Fax: 847-205-3804, e-mail: G15010@email.mot.com

INTRODUCTION

Bonds that exhibit very sharp and well-defined corners are found in electronic packages where features are accurately controlled and/or materials are dispensed in very small volumes. Typical examples would be a microchip encapsulated in a molding compound or a miniature leadless component surface-mounted with tiny dots of electrically-conductive adhesive. When these components are subjected to a cyclic thermo-mechanical loading, it has been observed that cracks tend to initiate at bimaterial interface corners.

In structural adhesive bonds, where spew fillets are generally not precisely controlled, surface contaminants during fabrication will cause the contact angle of the adhesive to be high locally. This type of defect may give rise to singular behavior, eventually leading to crack initiation if the applied load is high enough and if plasticity is limited, as in the case of fatigue loadings.

Fracture mechanics approaches to the prediction of adhesive bond durability under cyclic loading assume the presence of detectable initial crack-like flaws in the bond line, and determine the criticality and the propagation behavior of these flaws [1–3]. Under controlled fabrication conditions, however, such initial flaws may not be present within the high stress regions where fatigue damage initiates. Under these circumstances, the number of cycles to debond initiation rather than the cycles responsible for debond propagation may dominate the total life of the bonded structure [3].

Our approach is based on the observation that crack initiation occurs near the interface corners, where the stress fields are predicted to be singular [4, 5]. Hence, we define a fatigue initiation criterion using the concept of a generalized stress intensity factor derived from the mechanics of singular stress fields. Despite a significant interest in these singular stress fields and associated failure criteria, only limited experimental applications have been reported [6–11]. Several factors directly affect the applicability of these theoretical models to actual bonds. The size of the singular zone (herein shown to be on the order of 100 μm) is often smaller than the thickness of a typical bond line, and significantly smaller than the size of the spew region which is frequently formed in bonded joints. This implies that details of the spew region could dominate the results. Furthermore, the singular

stresses are predicted based on linear elasticity. The ability for even relatively brittle materials to yield locally in regions of high stresses does raise concerns about the applicability of the singularity approach. The lower stress levels and reduced plasticity encountered in fatigue loading is expected to improve the applicability of this approach, and provides motivation for this study.

In Part 1 of this paper, we first give a general presentation of the fatigue failure criterion in the context of metal-polymer bonds, and we define its range of applicability. Second, we analyze the special case of a wedge-shaped specimen loaded in bending. The bimaterial wedge specimen will be used in Part 2 [12] of this paper to determine experimentally the fatigue initiation envelope of an epoxy-aluminum bond.

SINGULAR STRESS FIELDS AT A METAL-POLYMER INTERFACE

Excluding the case of adherend corners embedded in a spew fillet (which will not be discussed in this study), an adhesive joint terminus is a special case of two dissimilar bonded wedges. A schematic of a double bonded wedge is given in Figure 1. Note that for a metal-to-polymer bond, we often have: $\phi_2 = 180°$ and $0° < \phi_1 < 90°$.

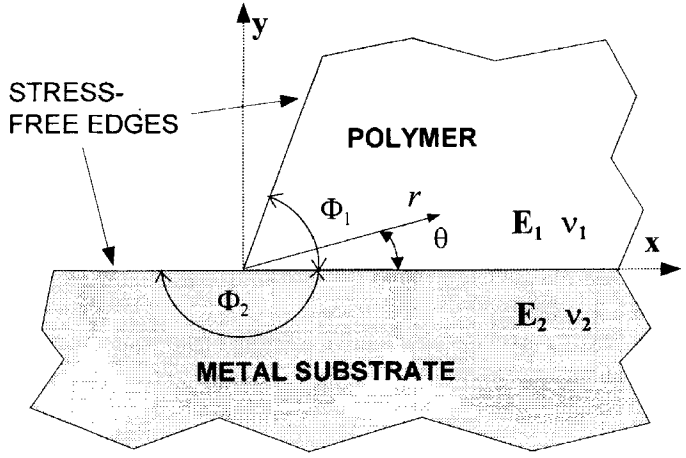

FIGURE 1 Dissimilar bonded wedges showing polar and cartesian coordinate systems.

Linear elasticity solutions for a bimaterial wedge subjected to some general loading are available in the literature [13, 14]. The stresses in the near field of the interface corner are singular and, in *polar coordinates*, are described as:

$$\sigma_{ij}(r,\theta) = \sum_{k=1}^{\infty} T_{ij}^{k}(\theta) r^{-\lambda_k} \tag{1}$$

$T_{ij}^{k}(\theta)$: Some function dependent on θ, load and geometry
r : Distance from singular point
λ_k : Eigenvalues

Eigenvalues λ_k can be calculated by solving a characteristic transcendental equation of the form [13]:

$$\begin{aligned} &A(\phi_1,\phi_2,P)\beta^2 + 2B(\phi_1,\phi_2,P)\alpha\beta + C(\phi_1,\phi_2,P)\alpha^2 \\ &\quad + 2D(\phi_1,\phi_2,P)\beta + 2E(\phi_1,\phi_2,P)\alpha + F(\phi_1,\phi_2,P) = 0 \end{aligned} \tag{2}$$

where P is determined by the roots of the Eigen function, A, B, C, D, E and F are auxiliary functions, and the Dundurs parameters α and β can be written using the following elastic parameters [6]:

$$\alpha = \frac{G_1 m_2 - G_2 m_1}{G_1 m_2 + G_2 m_1}, \quad \beta = \frac{G_1(m_2 - 2) - G_2(m_1 - 2)}{G_1 m_2 + G_2 m_1},$$

with:

$$m_\xi = \frac{4}{(1+\nu_\xi)} \quad \text{for plane stress,}$$

$$m_\xi = 4(1-\nu_\xi) \quad \text{for plane strain,}$$

$$G_\xi = \frac{E_\xi}{2(1+\nu_\xi)},$$

E_ξ, ν_ξ, are the moduli and Poisson's ratios respectively, and $\xi = 1, 2$ for the two materials.

Eigenvalues λ_k can be obtained by finding the real part of eigenvalues P_k of Eq. (2) and using the relationship:

$$\lambda_k = 1 - P_k \tag{3}$$

with: $0 < \mathrm{Re}(\lambda_k) < 1$ (see Ref. [13]).

λ_k can be real or complex. For $\mathrm{Re}(\lambda_k) > 0$, a stress singularity exists. In addition, $\lambda_k = 0$ is always a solution, leading to a non-singular stress term independent of r. Often, when Eq. (2) has several real singular roots, the largest λ_k is used as the order of the singularity. With complex roots, the largest real part of Eq. (3) is used. It is frequently argued that the highest value of λ_k dominates the stress field near the singular point [14]. Caution should be used when considering this approximation, however. For example, Groth [15], pointed out that in the case of an adherend corner embedded in a fillet, the "effective" λ that best approximates the stress field near the corner can be very different from the largest real root of the characteristic equation.

FATIGUE INITIATION CRITERION

Background

Using the plane strain[1] formulation of Eq. (2), we calculated the non-zero values of λ_k in the case of a flat metal substrate. The solution was obtained for a wide range of modulus ratios (polymer-to-metal) and assuming that the Poisson's ratio of the two materials was equal to 0.3. The results are summarized in Figure 2 representing λ_k as a function of wedge angle. Whenever $E_1/E_2 < 1$, each curve can be divided into 3 regions from left to right. In the first segment, Eq. (2) has a single real root. In the second segment, at intermediate angles, Eq. (2) has two real roots. In the third segment, Eq. (2) has a single complex root, and we plotted its real part. When $E_1/E_2 = 1$ (no mismatch in elastic properties), Eq. (2) has no complex root.

It should be noted that there is no positive critical angle below which the singularity completely disappears. Although, for a modulus ratio of 0.001, the eigenvalue seems to vanish at some finite angle on a full-scale plot, our numerical results clearly indicate that λ does not really go to zero until a wedge angle of 0° is reached.

---

[1]Knowing that typical adherends are plate-shaped, we used the plane strain assumption in the general discussion of the failure criterion. When discussing the special case of a narrow bimaterial wedge specimen, however, we used the plane stress assumption.

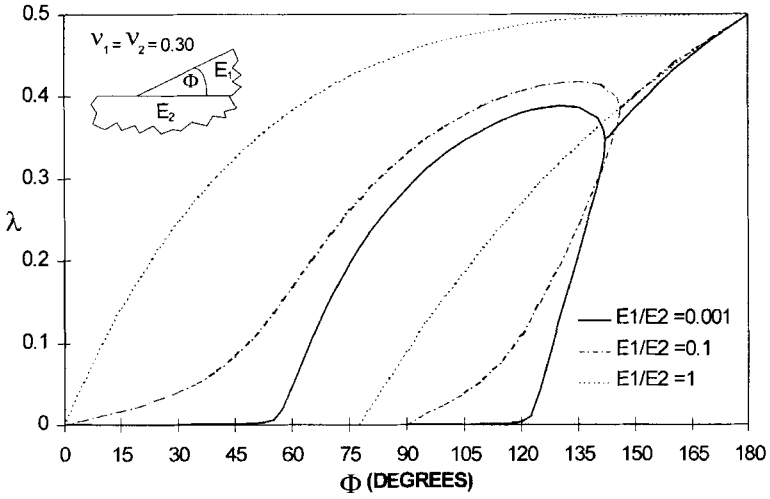

FIGURE 2 Wedge bonded to a flat substrate. Effect of the modulus ratio on the real part of the eigenvalue (plane strain).

In the double real root region (whose angular range varies with modulus ratio) it can be shown that Eq. (1) reduces to two singular terms and a term independent of r [16]:

$$\begin{aligned}
\sigma_r &= \frac{K_1}{r^{\lambda_1}} f_{\xi r}^1(\theta) + \frac{K_2}{r^{\lambda_2}} f_{\xi r}^2(\theta) + K_0 f_{\xi r0}(\theta) \\
\sigma_\theta &= \frac{K_1}{r^{\lambda_1}} f_{\xi\theta}^1(\theta) + \frac{K_2}{r^{\lambda_2}} f_{\xi\theta}^2(\theta) + K_0 f_{\xi\theta0}(\theta) \\
\tau_{r\theta} &= \frac{K_1}{r^{\lambda_1}} f_{\xi r\theta}^1(\theta) + \frac{K_2}{r^{\lambda_2}} f_{\xi r\theta}^2(\theta) + K_0 f_{\xi r\theta0}(\theta)
\end{aligned} \tag{4}$$

where $f_{\xi ij}^{\zeta}(\theta)$ are angular functions, with: $\xi = 1, 2$ for the two materials. K_1 and K_2 are generalized stress intensity factors, dependent on boundary conditions. It should be noted that since no geometric symmetry can be found when the substrate is flat (and the wedge angle is smaller than 180°), K_1 and K_2 do *not*, in general, refer to mode I and mode II deformation.

The angular functions are only dependent on the elastic constants and the angle, but are independent of loading conditions. Analytical expressions for the angular functions in the case of the free edge of a

bimaterial interface are given in Ref. [16]. The constant stress terms need to be taken into account in the case of a thermal loading or in the case of edge traction [16] but may be neglected in other cases.

It is important to note that when a thermal loading or edge traction are present, K_1 and K_2 also receive contributions from these two types of loadings [16]:

$$K_\zeta = K_\zeta^R + K_\zeta^T + K_\zeta^{\mathrm{Th}} \tag{5}$$

where superscripts, R, T and Th stand for "Remote loading", "Edge Traction", and "Thermal", respectively, and $\zeta = 1$ or 2 for the two intensity factors.

Near the edge, constant term K_0 Eq. (4) arising from the three types of loadings described above becomes negligible. This term does not contribute to the singular behavior, and for the purpose of the failure analysis, can be considered together with the far field terms.

When Eq. (2) has one real root, Eq. (4) has only one singular term. By considering the stresses along the bimaterial interface ($\theta \to 0$), and going to *Cartesian coordinates* (see Fig. 1 for a definition of the axes), the singular part of Eq. (4) can be simplified. Using the notation introduced by Groth [4], the singular stresses may be written as:

$$\sigma_{kl} = \frac{Q_{kl}}{x^\lambda} \tag{6}$$

Although Q_{kl} is clearly mathematically different from K_ζ because it factors in the angular functions, we will also refer to this parameter as a generalized stress intensity factor, because it essentially has the same physical meaning. Examining Eq. (4), one can see that for a given bimaterial wedge, and provided that the solution to Eq. (2) lies in the single root region, ratios Q_{xy}/Q_{yy} and Q_{xx}/Q_{yy} are independent of boundary conditions. This means that in principle, *any Q_{kl} can be used as a failure criterion interchangeably.*

Several authors [4, 5, 6, 7, 9] have utilized parameter Q_{kl} as a "generalized" stress intensity factor suitable as a failure criterion for bonded dissimilar materials. Of special interest is the work of Hattori *et al.*, who used Q_{xy} calculated from the interfacial shear stress distribution as a failure criterion for encapsulated LSI (Large Scale

Integrated Circuit) devices subjected to thermal stresses [6]. The delamination criterion obtained by Hattori for a Fe-Ni alloy bonded to epoxy was a monotonically decreasing curve, with Q^c_{xy} (critical) as the ordinate, and λ as the abscissa. λ was varied by using various configurations of epoxy/Fe-Ni rectangular blocks bonded together. Q_{xy} was calculated by best fitting Eq. (6) to the σ_{xy} distribution, which had been computed using Finite Element Analysis. Hattori *et al.*, obtained Q^c_{xy} by measuring the critical thermal shear stress leading to delamination. Remarkably, the failure criterion obtained from thermally-loaded samples was in fair agreement with the Goland and Reissner prediction of the failure strength of single lap joints made of the same metal-polymer combination [7].

Hattori did not appear to check whether the single root condition was satisfied in all cases. Our calculations have shown that for one geometry used by Hattori, Eq. (2) yielded two real roots. However, because one root was negligible compared with the other, the author was justified in using Q_{xy} as a failure criterion.

The special case of an homogeneous notched material ($E_1 = E_2$, $\nu_1 = \nu_2$, $\phi_1 = \phi_2$) has also been investigated [17]. The material was PMMA, and the concept of critical stress intensity factor was used successfully.

Maximum Wedge Angle Yielding a Single Root

Since the maximum wedge angle yielding a single root in Eq. (2) dictates whether or not a single Q_{kl} can be used as a failure criterion, we calculated it as a function of modulus ratio, using Eq. (2). The results are shown in Figure 3, for the general case of a wedge bonded to a flat substrate. For the sake of convenience, both Poisson's ratios were assumed to be equal to 0.3.

It can be seen that for an infinitely rigid substrate, the maximum angle is 90°, and remains so for a modulus ratio as high as 0.1. Above 0.1, the maximum wedge angle yielding a single root decreases exponentially with the modulus ratio.

Since the modulus ratio is less than 0.1 for the most common polymer-to-metal bonds, and since the free edge of the adhesive usually intersects the surface of the substrate at an angle, comprised between 0° (fillet with perfect wetting) and 90° (molded or machined corner), we

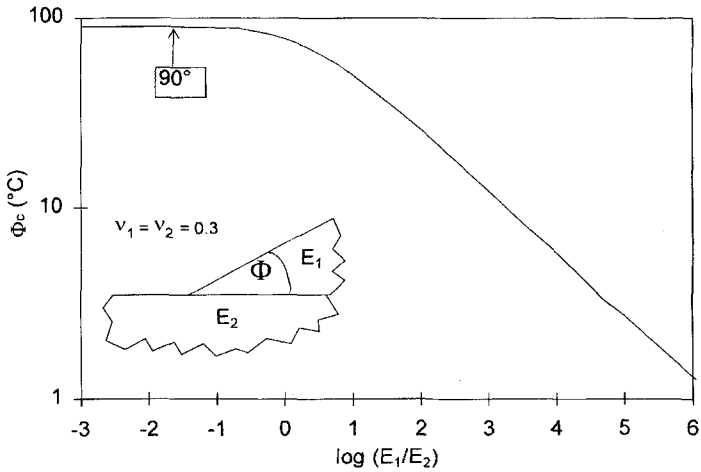

FIGURE 3 Maximum wedge angle yielding a single-root solution *vs.* modulus ratio (plane strain). The Poisson's ratios are assumed to be both equal to 0.3.

conclude that for a given polymer contact angle, *a single generalized Q^c is a valid failure criterion in most cases of polymer-to-metal adhesion.*

The fact that most polymer-to-metal bonds allow use a single Q^c is of considerable practical interest. If one had to consider the case of multiple roots, one would need to use both K_1 and K_2 as failure criteria. This would be very inconvenient because the determination of two intensity factors requires much computation [18], and would introduce a third dimension to the failure criterion.

Definition of the Fatigue Initiation Criterion

The fatigue initiation criterion used in this study is a generalization of Hattori's. To the two axes of Hattori's criterion (λ and Q), we simply added a third axis corresponding to the number of cycles to initiation (N_i). We thereby defined a 3-D delamination envelope. For $N_i = 1/4$, the envelope reduces to Hattori's 2-D criterion. For a fixed value of λ ($\lambda > 0$), the Q *vs.* N_i plot is reminiscent of the classical S-N curve, as is exactly the case for $\lambda \to 0^+$. Since we limit λ to the single-root region, another possible representation of the failure criterion is to replace λ by the corresponding values of the adhesive angle varying from 0° to 90°. This concept is illustrated in Figure 4.

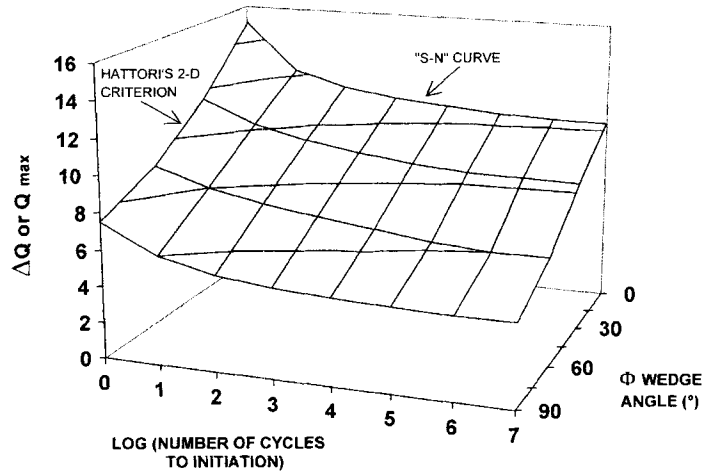

FIGURE 4 Fictitious example of fatigue initiation criterion for a given bimaterial system (experimentally determined). Note that the 3-*D* representation is possible only as long as a single intensity factor can be used as a failure criterion. The vertical axis may be used to plot either ΔQ or Q_{max}. The surface must be experimentally determined and is specific to a given bimaterial system (and associated surface treatment, *etc.*).

THE SPECIAL CASE OF AN EPOXY-TO-ALUMINUM WEDGE SPECIMEN

The Bimaterial Wedge Specimen

A bimaterial wedge specimen was specifically designed to obtain experimentally 3-*D* fatigue initiation envelopes in Part 2 of this work [12]. The specimens are loaded in bending in a cantilever configuration. λ and Q are controlled by varying the wedge angle and the applied force, respectively. Crack initiation is monitored using strain gages located near the wedge tip. Figure 5 illustrates the wedge geometries and the boundary conditions used in the numerical analysis. For a description of the experimental set-up and of the actual specimen dimensions, the reader is referred to the experimental part of this paper [12]. The goals of the specimen analysis were three-fold:

- Optimize the wedge angles from the λ *vs.* wedge angle curve.
- Assess the size of the region dominated by the singularity.
- Develop a methodology for wedge specimen calibration (Q *vs.* applied load). Calibration will be needed in Part 2 of this paper [12].

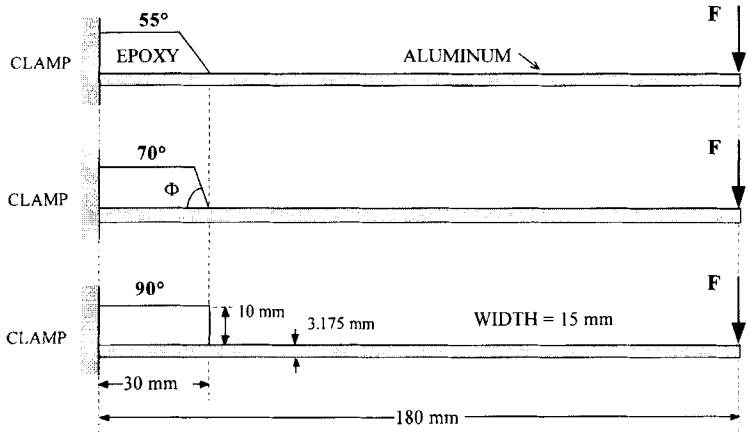

FIGURE 5 Wedge specimens: boundary conditions.

Analytical Solution of λ *vs.* Wedge Angle

Using the plane stress formulation[2] of Eq. (2), we calculated the non-zero values of λ_k, first in the case of an epoxy wedge bonded to a flat aluminum substrate and, second, in the case of an aluminum wedge bonded to a flat epoxy substrate. The elastic properties of the aluminum were $E_1 = 69$ GPa and $\nu_1 = 0.3$. The elastic properties of the epoxy used in Part 2 were $E_2 = 3.2$ GPa and $\nu_2 = 0.35$. The results are summarized in Figure 6, representing λ as a function of wedge angle.

From Figure 6, it can be readily seen that the best way to vary λ experimentally *via* the wedge angle is to use an epoxy wedge bonded to a flat aluminum substrate. This is also the case most relevant to real bonded joints. The opposite configuration is impractical, because λ varies from 0 to 0.5 within a very narrow range of wedge angles. This result was experimentally verified by Voloshin *et al.* [19], using Moiré interferometry on aluminum and acrylic wedges bonded to substrates made of the opposite materials.

[2]Note that the plane stress assumption is reasonable throughout most of the specimen, except locally on the polymer side of the apex, where transverse strains are constrained by both the surrounding polymer and substrate. To resolve this ambiguity completely, one would have to perform a 3-*D* analysis.

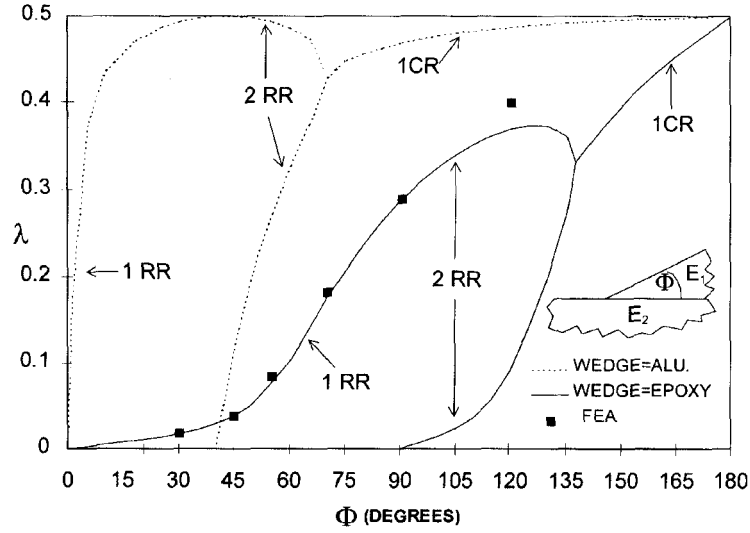

FIGURE 6 Order of singularity *vs.* wedge angle, plane stress analytical solution. 1 RR: 1 Real Root. 2 RR: 2 Real Roots. 1 CR: 1 Complex Root.

Finite Element Analysis

2-*D* linear elastic, plane-stress, finite element modeling of the wedge specimens was performed with ABAQUS, using 8-node quadratic elements. Within the design deflection range, non-linear geometric analysis was not found to be necessary. The boundary conditions are shown in Figure 5.

In order to capture the singular behavior, meshes near the wedge tip were extremely refined. Figure 7 illustrates the mesh used for the tip of the 70° wedge specimen. With 20 quadratic elements in the radial direction around the tip, and a bias of 0.70, we obtained a node size of the order of 10^{-5} mm at the apex of the wedge. The same mesh pattern around the tip was used for all angles studied.

Interfacial Peel Stress Distribution

The calculated distribution of interfacial peel stress, σ_{yy}, in the vicinity of the wedge apex is shown on a log–log scale in Figure 8. σ_{yy} was normalized with respect to the bending moment acting on the beam

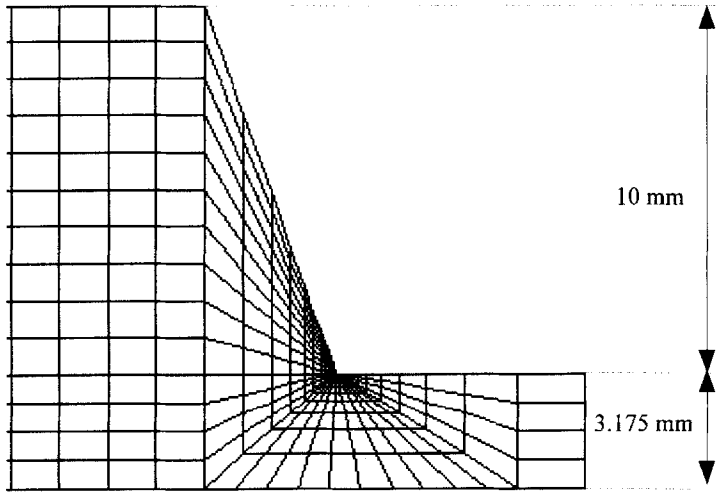

FIGURE 7 Mesh used to model the 70° wedge specimen. The size of the elements around the tip is of the order of 10^{-5} mm.

section located right under the apex (the vertical shear force acting on this beam section was ignored, because its effect on Q is insignificant). Five angles were studied numerically: 45°, 55°, 70°, 90° and 120°. The σ_{yy} stress distribution follows Eq. (1) as far as 10^{-1} mm from the tip, and then drops rapidly. This is due to the fact that the epoxy acts as an elastic foundation for the aluminum beam, thus giving rise to an oscillatory far-field behavior.

The σ_{yy} stress distribution was also calculated along all the rays around the wedge tip. The obtained values of λ as a function of angular position are shown in Figure 9. λ is independent of angular position. The small variations seen in Figure 9 are simply due to the numerical approximation.

A comparison of the analytical and numerical predictions of λ *vs.* wedge angle can be seen in Figure 6. The plane-stress solutions of Eq. (2) are compared with the plane-stress finite element predictions. Note that within the single root region (up to 90°), the numerical and analytical solutions are in excellent agreement. This is no longer true in the double root region (*e.g.*, 120° wedge). This is expected, because curve-fitting the stress distribution from FEA to a single singular

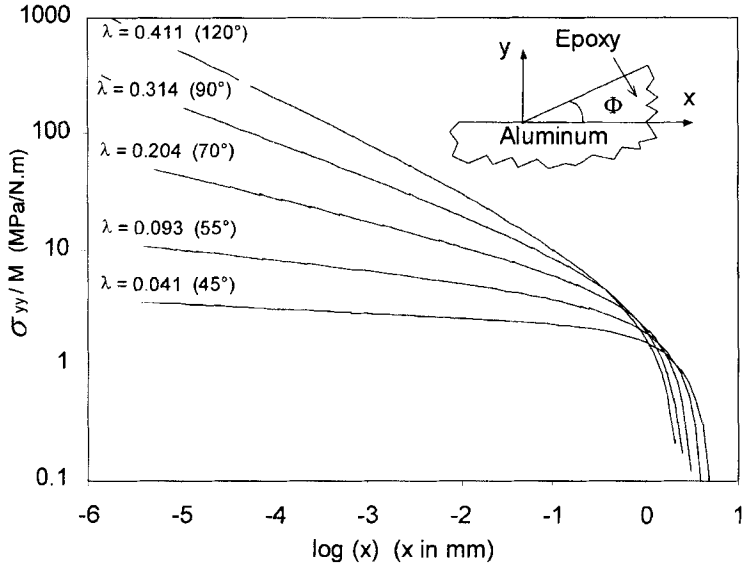

FIGURE 8 Normalized interfacial peel stress distribution near the apex for several wedge angles (plane stress 2-*D* analysis).

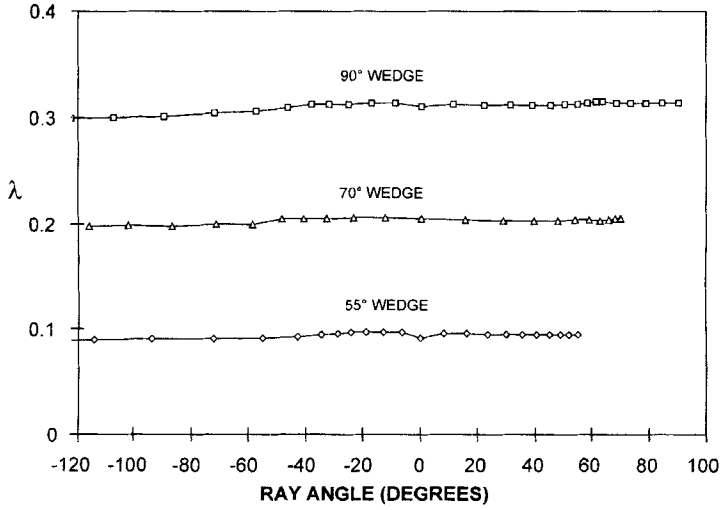

FIGURE 9 λ *vs.* angular position around the apex. Plane stress finite element predictions. λ was calculated from the peel stress distribution.

term yields an "effective" λ that is not necessarily close to λ_{max} [15]. A summary of the eigenvalues obtained analytically from finite element analysis, for a ray angle of 0° (interface), is given in Table I.

Size of the Singular Region for the Selected Specimen Geometry

The boundary of the region dominated by the singular field was arbitrarily defined as follows: On a log–log scale, the linear (singular) portion of the stress distribution from the apex (asymptote) was extrapolated to larger distances. The boundary was the distance from the apex, such that the difference between the stress and the singular asymptote was equal to 0.05 on the log–log scale. This procedure was repeated along each ray. Two measures of stress were used to define the boundary: Von Mises and the maximum principal stress.

A map of the singular region for a 55° wedge is shown in Figure 10. It can be seen that for the two stress definitions used, the singular zone is almost the same. Its size along the interface is of the order of 100 μm. The same result was found for a 90° angle. Because theory predicts that the size of the singular zone is dependent on the far field stress, the obtained values are indicative only. Nonetheless, we found that in the range of wedge angles investigated, the size of the singular region at the interface was nearly constant.

For the stress singularity approach to be applicable to failure prediction, the size of the singular zone should be significantly larger than the fracture process zone, intrinsic flaw size, plastic yield zone [9], and geometric imperfections at the apex. This means that in the experimental part of this work, we should strive to fabricate specimens with a tip sharpness smaller than 100 μm.

TABLE I Comparison of the eigenvalues obtained analytically and by Finite Element Analysis (plane stress). The numerically-obtained eigenvalues are averages from the values obtained from the peel and shear stress distributions along the bimaterial interface

Wedge angle	55°	70°	90°
λ (Analytical)	0.08	0.18	0.29
λ (Numerical)	0.09	0.19	0.30

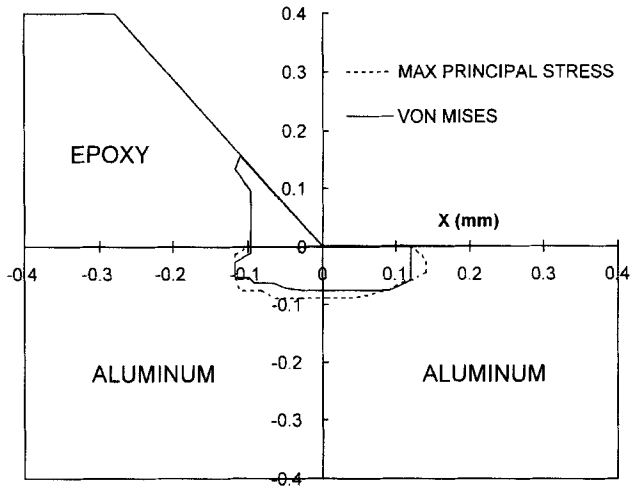

FIGURE 10 Map of the singular region for a 55° wedge specimen (From plane stress finite element analysis). The size of the singular zone is comparable for 70° and 90° wedge angles.

Additional finite element analysis revealed that for a given bimaterial system and wedge angle, the size of the singular zone scales linearly with the dimensions of the specimen. This is illustrated in Figure 11 in the case of a fictitious 55° bimaterial wedge specimen whose dimensions were varied isotropically over 4 orders of magnitudes.

As pointed out earlier, a key assumption of the fatigue initiation criterion is that the plastic zone or geometrical defects near the apex be significantly smaller than the singular region. When designing a specimen for the purpose of obtaining a singularity-based failure criterion, it may, therefore, be advantageous in some cases to increase the specimen size. This would be particularly true when ductile adhesives are used, or when the cost of manufacturing corners with a sharpness tolerance significantly smaller than 100 μm is prohibitive.

On the contrary, when designing a structure with the objective of eliminating singular behavior, the above results indicate that, in addition to using a more ductile adhesive or rounding off corners, one also has the option of reducing adhesive or adherend dimensions. In the case of structural adhesives, for example, it would be advantageous to reduce bond line thickness until the plastically-yielded zone becomes larger than the singular zone.

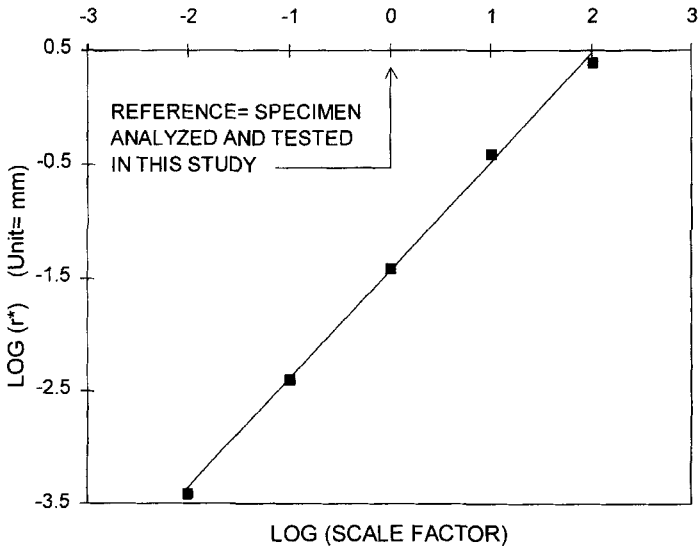

FIGURE 11 Dimension of the singular zone r^* *vs.* scale factor (From Finite Element Analysis). The reference geometry was a 55° bimaterial wedge and the dimension of the singular zone was defined along the aluminum-epoxy interface.

ESTIMATION OF THE SIZE OF THE PLASTIC YIELD ZONE

For a given polymer, the maximum possible size of the plastic yield zone generated at the apex of the wedge can be estimated with the following expression [20]:

$$r_p = \gamma \left(\frac{Q^c_{\mathrm{VM}}}{\sigma_{yd}} \right)^{1/\lambda} \tag{7}$$

where:

r_p = Radius of the plastic zone
$Q^c_{\mathrm{VM}} = Q^c$ calculated from the Von Mises stress distribution (Q^c is the critical value of the stress intensity factor)
σ_{yd} = Yield strength of the polymer
λ = Order of the singularity
γ = Assumption-dependent coefficient.

For a lower-bound estimate based on a linear elastic solution [20], $\gamma = 1$. For a more conservative estimate analogous to that of a crack tip yield zone [20], $\gamma = 2$.

The relationship between the size of the plastic zone and parameters Q^c and σ_{yd} is illustrated in Figure 12, in the case of a 90° epoxy-aluminum wedge specimen ($\lambda = 0.3$). Coefficient γ was assumed to be equal to 2. We can see that for the yield strength of our epoxy (83 MPa [21]), a Q^c as high as 20 MPa mm$^{\lambda}$ will give a plastic zone almost an order of magnitude smaller than the singular zone. More importantly, we observe that for a given polymer yield strength, the plastic zone decreases exponentially as Q^c goes down. The exponent is equal to 3.3 in the case of a 90° wedge (Fig. 12). It is as high as 5 for a 70° wedge, and 10 for a 55° wedge. This rapid decrease means that even if the plastic zone is too large to apply the stress singularity approach at loads close to the static strength of the interface (high Q^c, low σ_{yd}, or both), it nonetheless has a good chance to be small enough at load levels associated with the fatigue limit. To insure that the singularity

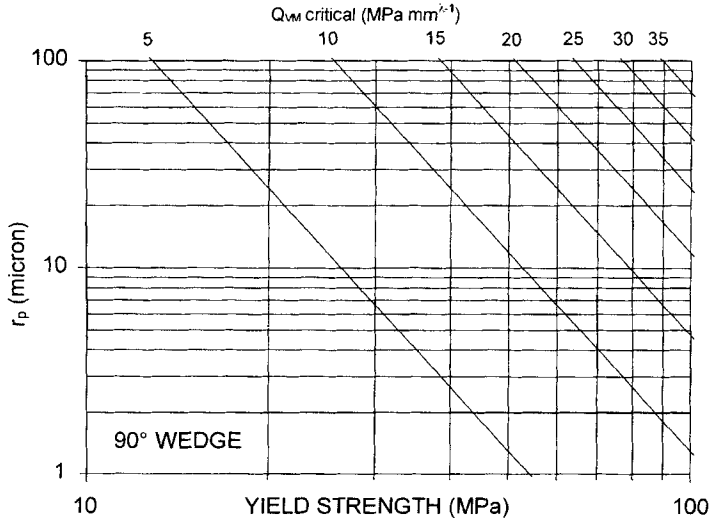

FIGURE 12 90° Wedge specimen: size of the plastic zone *vs.* yield strength of the epoxy, for selected values of Q^c calculated from the Von Mises interfacial stress distribution ($\gamma = 2$).

approach is applicable, the above analysis should be repeated for every new case of bimaterial interface and wedge geometry.

CONCLUSIONS

For edge corner angles as high as 90° and for modulus ratios smaller than 0.1, a failure criterion independent of geometry and loading can be defined with a single generalized stress intensity factor. With a single generalized stress intensity factor, it is possible to generalize Hattori's 2-*D* static criterion to define a fatigue initiation surface. This surface is experimentally determined and is characteristic of a given bimaterial system.

For the stress singularity approach to be applicable, the size of the singular zone has to be larger than that of the fracture process zone, intrinsic flaw size, plastic yield zone [9], and geometric imperfections at the apex. For a given polymer yield strength, the size the plastic zone decreases extremely rapidly as Q^c goes down. This suggests that we are likely to encounter situations where the singularity approach is applicable near fatigue limit stress levels, despite an oversized plastic zone at stress levels corresponding to static failure.

The singular zone scales linearly with the dimensions of the structure. In the case of a conventional structural joint, this means that with a thin enough bond line, the plastic zone near the bimaterial corners can theoretically be made larger than the singular region, thereby blunting crack initiation.

Although a typical adhesive bond terminus does exhibit geometrical variations over the width of the overlap, it is locally, where the apex is sharpest, that initiation will tend to take place. Thus, the use of an idealized geometry can be useful to obtain conservative estimates of the fatigue life-to-initiation of structural adhesive bonds.

In the field of electronic packaging, bimaterial interface corners are typically very sharp. This characteristic, combined with the fact that chip encapsulants and conductive adhesives are usually highly-filled, brittle materials, makes the stress singularity approach very attractive. Possible applications include durability predictions and design improvements for electronic components subjected to fatigue loadings arising from mechanical, thermal, or hygroscopic cycling.

Acknowledgments

This work was funded by the National Science Foundation Science and Technology Center: High Performance Polymeric Adhesives and Composites, contract DMR 9120004. The authors express thanks to E. Reedy from Sandia National Labs and to R. Andruet from Virginia Tech for helpful discussions.

References

[1] Kinloch, A. J. and Osiyemi, S. O., *J. Adhesion* **43**, 79 (1993).
[2] Kinloch, A. J., *Proceedings of the Institution of Mechanical Engineers, 84th* Thomas Hawksley Memorial Lecture, London, Dec. 1996.
[3] Shang, J. K. and Chernenkoff, R. A., In: *SAE Technical Paper Series* **960575**, (International Congress & Exposition, Detroit, Michigan, 1996).
[4] Groth, H. L., *Int. J. Adhesion and Adhesives* **8**, 107 (1988).
[5] Adams, R. D. and Harris, J. A., *Int. J. Adhesion and Adhesives* **7**, 69 (1987).
[6] Hattori, T., Sakata, S. and Murakami, G., *J. Electronic Packaging* **111**, 243 (1989).
[7] Hattori, T., *JSME International Journal*, Series I, **34**, 326 (1991).
[8] Reedy, E. D. and Guess, T. R., *Int. J. Solids Structures* **30**, 2929 (1993).
[9] Reedy, E. D. and Guess, T. R., *J. Adhesion Sci. Technol.* **9**, 237 (1995).
[10] Reedy, E. D. and Guess, T. R., *Int. J. of Fracture* **81**, 269 (1996).
[11] Reedy, E. D. and Guess, T. R., *J. Adhesion Sci. Technol.* **10**, 33 (1996).
[12] Lefebvre, D. R., Dillard, D. A. and Dillard, J. G., "A Stress Singularity Approach for the Prediction of Fatigue Crack Initiation in Adhesive Bonds. PART 2: Experimental", Companion paper, this issue.
[13] Bogy, D. B., *J. Appl. Mechanics* **35**, 460 (1968).
[14] Hein, V. L. and Erdogan, F., *Int. J. Fracture Mech.* **7**, 317 (1971).
[15] Groth, H. L., *Int. J. Adhesion and Adhesives* **8**, 55 (1988).
[16] Yang, Y. Y. and Munz, D., *Int. J. Solids Structures* **34**, 1199 (1997).
[17] Dunn, M. L., Suwito, W. and Cunningham, S., *Int. J. Structures* **34**, 3873 (1997).
[18] Munz, D. and Yang, Y. Y., *Int. Journal of Fracture* **60**, 169 (1993).
[19] Voloshin, A. S. and Tsai, L.-T., *Engineering Fracture Mechanics* **43**, 477 (1992).
[20] Reedy, E. D., *Int. J. Solids Structures* **30**, 767 (1993).
[21] Shell Technical Report "*Epon Resin, Epoxy Bisphenol F 862*", Shell Chemical Company (1995).